



Shamsudin, M., and York, C. (2014) *Mechanically coupled laminates with balanced plain weave*. *Composite Structures*, 107 . pp. 416-428. ISSN 0263-8223

Copyright © 2014 Elsevier

A copy can be downloaded for personal non-commercial research or study, without prior permission or charge

Content must not be changed in any way or reproduced in any format or medium without the formal permission of the copyright holder(s)

When referring to this work, full bibliographic details must be given

<http://eprints.gla.ac.uk/84161/>

Deposited on: 11 September 2013

Mechanically Coupled Laminates with Balanced Plain Weave

M H Shamsudin and C B York*

School of Engineering, University of Glasgow, University Avenue, G12 8QQ, Glasgow, Scotland.

Abstract

Definitive listings of laminate stacking sequences are derived for balanced plain weave laminated materials, assuming each layer is composed of the same material with constant thickness throughout and that standard ply angle orientations 0, 90, and $\pm 45^\circ$ are adopted; consistent with industrial design practice. A single layer of balanced plain weave material is shown to be immune to thermal distortion following a standard high temperature manufacturing process, which implies that all laminates constructed of this material possess what is commonly referred to as the hygro-thermally curvature-stable or warp-free condition, irrespective of the individual ply orientations used or the laminate stacking sequence definition. A single uncoupled parent laminate class is shown to contain sub-groups with extensionally isotropic and fully isotropic properties that are invariant with off-axis orientation of the principal material axes with respect to the system or structural axes. By contrast a single mechanically coupled parent

* Corresponding author:

Tel: +44 (0)141 3304345, E-mail address: Christopher.York@Glasgow.ac.uk

1 laminate class is shown to give rise to seven unique forms of coupled laminate through
2
3 judicious off-axis orientation. Invariant off-axis properties are also identified in
4
5 coupled laminate designs. Finally, example calculations, abridged stacking sequence
6
7 listings and design data are presented.
8
9

10 11 12 13 **Keywords**

14 Balanced Plain Weave, Spread Tow, Hygro-Thermally Curvature-Stable, Warp-free.

15
16
17
18 **Uncoupled Laminates: Quasi-Homogeneous; Extensionally Isotropic; Fully Isotropic.**

19
20
21 **Coupled Laminates: Extension-Shearing; Extension-Bending; Extension-Twisting;**
22
23 **Shearing-Bending; Shearing-Twisting; Bending-Twisting.**
24
25
26
27
28
29
30
31
32
33
34
35
36
37
38
39
40
41
42
43
44
45
46
47
48
49
50
51
52
53
54
55
56
57
58
59
60
61
62
63
64
65

Nomenclature

- A**, A_{ij} = extensional stiffness matrix and its elements ($i,j = 1, 2, 6$).
- B**, B_{ij} = coupling stiffness matrix and its elements ($i,j = 1, 2, 6$).
- D**, D_{ij} = bending stiffness matrix and its elements ($i,j = 1, 2, 6$).
- $E_{1,2}$, G_{12} = in-plane Young's moduli and shear modulus.
- H = laminate thickness (= number of plies, $n \times$ ply thickness, t).
- $M_{x, y, xy}$ = moment resultants.
- $N_{x, y, xy}$ = force resultants.
- $\mathbf{M}^{\text{Thermal}}$ = thermal moment resultant vector (= $\{M_x^{\text{Thermal}}, M_y^{\text{Thermal}}, M_{xy}^{\text{Thermal}}\}^T$).
- $\mathbf{N}^{\text{Thermal}}$ = thermal force resultant vector (= $\{N_x^{\text{Thermal}}, N_y^{\text{Thermal}}, N_{xy}^{\text{Thermal}}\}^T$).
- Q_{ij} = reduced stiffness ($i,j = 1, 2, 6$).
- U_i = laminate invariant ($i = 1,2,3,4,5$)
- z_k = layer k interface distance from laminate mid-plane.
- $\alpha_{1,2}$, α_{Iso} = principal and isotropic coefficients of thermal expansion
- $\boldsymbol{\varepsilon}$ = vector of in-plane strains (= $\{\varepsilon_x, \varepsilon_y, \varepsilon_{xy}\}^T$).
- $\boldsymbol{\kappa}$ = vector of curvatures (= $\{\kappa_x, \kappa_y, \kappa_{xy}\}^T$).
- ν_{ij} = Poisson ratio ($i, j = 1, 2$)
- θ_k = ply orientation for layer k
- ξ_{1-4} = lamination parameters for extensional stiffness.
- ξ_{5-8} = lamination parameters for coupling stiffness.
- ξ_{9-12} = lamination parameters for bending stiffness.

1
2
3
4 **1. Introduction**
5
6

7 Composite laminates made from woven cloth materials are now commonplace in
8 secondary structure applications, e.g. flight control surfaces, and are noteworthy for
9 their improved damage tolerance compared with their unidirectional material
10 counterparts. They are however most often used in their simplest form, i.e. balanced and
11 symmetric laminates, to mimic the metallic materials that they are replacing, which
12 serves only as a weight reducing strategy. Laminate tailoring using woven cloth
13 material offers the possibility of adding additional functionality to the material,
14 alongside weight reduction, by introducing unique mechanical interactions between in-
15 plane and out-of-plane deformations; a tailoring strategy which has been gaining
16 increasing momentum in recent years. For instance, Nixon [1] used plain weave
17 material to achieve mechanical Extension-Twisting coupling response in a tilt rotor
18 blade design. This laminate design concept was first discovered by Winckler [2], who
19 describes how Extension-Shearing coupling at the laminate level can be applied at the
20 structural or blade level to produce an Extension-Twisting response.
21
22
23
24
25
26
27
28
29
30
31
32
33
34
35
36
37
38
39
40
41

42 Recent work on the classification of coupled laminates [3] has identified 24 distinct
43 classes, containing all possible interactions between Extension, Shearing, Bending and
44 Twisting. These laminate classes were derived for unidirectional material using
45 combinations of standard fibre angle orientations, i.e. 0, 90 and/or $\pm 45^\circ$. However, a
46 major challenge restricting the widespread use of these mechanically coupled laminates
47 is the complicating issue of thermal warping distortion, which occurs on cooling after
48 the elevated temperature curing process used in the manufacture of high strength fibre-
49
50
51
52
53
54
55
56
57
58
59
60
61
62
63
64
65

1 epoxy material systems. Specially curved tooling is generally required to counteract
2 these warping distortions, often at great expense. Laminate tailoring, to achieve the
3
4
5
6
7
8
9
10
11
12
13
14
15
16
17
18
19
20
21
22
23
24
25
26
27
28
29
30
31
32
33
34
35
36
37
38
39
40
41
42
43
44
45
46
47
48
49
50
51
52
53
54
55
56
57
58
59
60
61
62
63
64
65

Lamination parameters, developed originally by Tsai and Hahn [4], represent ply angle dependent non-dimensional parameters, which relate to laminate stiffness properties and to non-mechanical force and moment resultants. These parameters have had a major influence on subsequent developments in HTCS laminate design by Chen [5] and Cross et al. [6], assuming uniform temperature and/or moisture change. Diaconu and Sekine [7] extended these lamination parameter relationships to account for linear through thickness variation of temperature and/or moisture. However, the correct equations are to be found in an erratum [8], which inspired Weaver [9] to derive the uniform temperature case; independently confirming the findings of others [4,5]. It should be noted that moisture equilibrium is achieved over an extended time period and with uncertainties regarding the uniformity of distribution, whereas in thin laminate construction, a uniform temperature state is achieved almost instantaneously. Indeed, the case of uniform temperature change has been revisited more recently, demonstrating [10] the entire range of mechanical coupling mechanisms that can be achieved with immunity to thermal warping distortion, and [11] presenting useful design rules, including suggestions for broader application to woven cloth materials.

A single layer of plain weave material is known to possess thermal stability, i.e., immunity to thermal warping distortion. This can be understood from physical reasoning alone, where equal numbers of identical warp and weft fibres exist within a single layer, thus representing an architecture described as square symmetric [4], i.e.,

1 with equal stiffness on principal axes. Woven cloth architectures with square
2 symmetric properties are generally classified as symmetric, as in plain weave, 2×2
3 twill weave, or 4×4 twill weave, etc. Non-symmetric woven cloth architectures, e.g. 5-
4 harness satin weave, have warp-dominated fibres on one side of the geometric mid-
5 plane and weft-dominated fibres on the other. A single layer of non-symmetric woven
6 cloth possesses coupling between in-plane and out-of-plane deformation, hence thermal
7 warping distortions arise in such architectures [12].

8
9
10
11
12
13
14
15
16
17
18 **Balanced plain weave architecture, illustrated in Fig. 1, can be characterized as a high**
19 **crimp fabric, where the crimp angle is typically of the order of 45° . Micro-mechanical**
20 **modelling [13-15] has helped in understanding the mechanisms leading to observed**
21 **reductions in elastic properties and mechanical performance in such high crimp fabrics,**
22 **compared to non-crimp fabric or unidirectional laminated material (see Table 1).**
23 **However, micro-mechanical modelling is generally based on a single layer, or lamina,**
24 **and on the basis of a representative volume element; multi-layer models are more**
25 **realistic within the context of the current article, and have for instance demonstrated the**
26 **importance of incorporating random phase shift [16] in the relative weave position**
27 **between layers, but such modelling strategies quickly approach current computational**
28 **limits. Indeed, present lamina level micro-mechanical modelling strategies have been**
29 **shown [17] to incorrectly predict the laminate level elastic properties; the significant**
30 **differences in elastic properties between a single layer and 8-layer balanced plain weave**
31 **laminate have been demonstrated experimentally [18]. Indeed it has been observed that**
32 **elastic modulus increases, with increasing number of layers, up to an asymptotic value**
33 **corresponding to the 8-layer balanced plain weave laminate [17].**
34
35
36
37
38
39
40
41
42
43
44
45
46
47
48
49
50
51
52
53
54
55
56
57
58
59
60
61
62
63
64
65

1 Straighter load-carrying fibres are present in satin and twill weave architecture, which
2
3 give rise to improved mechanical performance in comparison to plain weave. However,
4
5 such weave patterns violate the macro-mechanical assumption made in this study, i.e.,
6
7 that individual layers are specially orthotropic. Indeed, satin weave architecture has
8
9 been shown [12] to lead to significant thermal warping distortions in individual layers,
10
11 which is only mitigated through the use of special lamination strategies.
12
13

14
15 Spread tow, or thin ply reinforcement offers an enabling technology for enhanced
16
17 mechanical performance in plain weave architecture (TeXtreme[®]), without the ply-level
18
19 thermal instability of satin and twill weaves. Balanced plain weave architecture can
20
21 now be achieved with crimp angles as small as 2.5° by weaving flat tapes, rather than
22
23 yarns, where tape widths of 20mm and tape thicknesses of 70µm result in properties
24
25 approaching those of non-crimp fabric.
26
27

28
29 This study is limited to the assumption of specially orthotropic layers of woven cloth
30
31 material; specifically, symmetric or plain weave. Hence the classification of coupled
32
33 laminates in this category may be derived from the assumption of equal modulus ($E_1 =$
34
35 E_2) in the two orthogonal in-plane directions, and which can be verified experimentally
36
37 (see Table 1), with the added restrictions that each layer in the laminate has identical
38
39 material properties and thickness, and that layers differ only by their orientation.
40
41
42
43
44
45

46
47 The governing equations describing the physical behaviour and specific characteristics
48
49 of balanced plain weave laminates are developed in section 2. Section 3 highlights
50
51 special stiffness relationships for both uncoupled and coupled laminates with balanced
52
53 plain weave and summarises the number of laminate solutions with standard ply angles.
54
55 Comparisons for Extension-Twisting coupled laminate designs with unidirectional and
56
57 balanced plain weave materials are presented in section 4 before conclusions are drawn
58
59
60
61
62

in section 5. Finally, an appendix is provided, containing: a summary of laminate characterisation and; abridged stacking sequence listings with design parameters for uncoupled and coupled laminates with balanced plain weave architecture.

2. Laminate Characterisation

Coupled laminates may be classified by either a suitable description of the form of the

ABD stiffness matrix, i.e.:

$$\begin{aligned}
 \begin{Bmatrix} N_x + N_x^{\text{Thermal}} \\ N_y + N_y^{\text{Thermal}} \\ N_{xy} + N_{xy}^{\text{Thermal}} \end{Bmatrix} &= \begin{bmatrix} A_{11} & A_{12} & A_{16} \\ A_{12} & A_{22} & A_{26} \\ A_{16} & A_{26} & A_{66} \end{bmatrix} \begin{Bmatrix} \varepsilon_x \\ \varepsilon_y \\ \gamma_{xy} \end{Bmatrix} + \begin{bmatrix} B_{11} & B_{12} & B_{16} \\ B_{12} & B_{22} & B_{26} \\ B_{16} & B_{26} & B_{66} \end{bmatrix} \begin{Bmatrix} \kappa_x \\ \kappa_y \\ \kappa_{xy} \end{Bmatrix} \\
 \begin{Bmatrix} M_x + M_x^{\text{Thermal}} \\ M_y + M_y^{\text{Thermal}} \\ M_{xy} + M_{xy}^{\text{Thermal}} \end{Bmatrix} &= \begin{bmatrix} B_{11} & B_{12} & B_{16} \\ B_{12} & B_{22} & B_{26} \\ B_{16} & B_{26} & B_{66} \end{bmatrix} \begin{Bmatrix} \varepsilon_x \\ \varepsilon_y \\ \gamma_{xy} \end{Bmatrix} + \begin{bmatrix} D_{11} & D_{12} & D_{16} \\ D_{12} & D_{22} & D_{26} \\ D_{16} & D_{26} & D_{66} \end{bmatrix} \begin{Bmatrix} \kappa_x \\ \kappa_y \\ \kappa_{xy} \end{Bmatrix}
 \end{aligned} \tag{1}$$

or, by a description of the physical response, due to an applied set of force and/or moment resultants. The two classifications are complementary and are therefore both employed here to provide additional insight. In the first case, the Engineering Sciences Data Unit [19] subscript notation is used, with suitable augmentation, to describe the exact form of the elements in the extensional [**A**], coupling [**B**], and bending [**D**] stiffness matrices, which in turn relate to the precise form of coupling behaviour of the laminate. In the second case, a *cause-effect* response based labelling system is adopted [3]. Detailed comparisons of both systems are provided in the appendix (Table A1).

The elements of the **ABD** matrix in Eq. (1) can be calculated from the (independent) laminate invariants, U_i ($i = 1, \dots, 5$), and lamination parameters, ξ_j ($j = 1, \dots, 12$):

$$\begin{aligned}
A_{11} &= (U_1 + \xi_5 U_2 + \xi_2 U_3) H & B_{11} &= (\xi_5 U_2 + \xi_6 U_3) H^2 / 4 & D_{11} &= (U_1 + \xi_9 U_2 + \xi_{10} U_3) H^3 / 12 \\
A_{12} = A_{21} &= (-\xi_2 U_3 + U_4) H & B_{12} = B_{21} &= (-\xi_6 U_3) H^2 / 4 & D_{12} = D_{21} &= (U_4 - \xi_{10} U_3) H^3 / 12 \\
A_{16} = A_{61} &= (\xi_3 U_2 / 2 + \xi_4 U_3) H & B_{16} = B_{61} &= (\xi_7 U_2 / 2 + \xi_8 U_3) H^2 / 4 & D_{16} = D_{61} &= (\xi_{11} U_2 / 2 + \xi_{12} U_3) H^3 / 12 \\
A_{22} &= (U_1 - \xi_1 U_2 + \xi_2 U_3) H & B_{22} &= (-\xi_5 U_2 + \xi_6 U_3) H^2 / 4 & D_{22} &= (U_1 - \xi_9 U_2 + \xi_{10} U_3) H^3 / 12 \\
A_{26} = A_{62} &= (\xi_3 U_2 / 2 - \xi_4 U_3) H & B_{26} = B_{62} &= (\xi_7 U_2 / 2 - \xi_8 U_3) H^2 / 4 & D_{26} = D_{62} &= (\xi_{11} U_2 / 2 - \xi_{12} U_3) H^3 / 12 \\
A_{66} &= (-\xi_2 U_3 + U_5) H & B_{66} &= (-\xi_6 U_3) H^2 / 4 & D_{66} &= (-\xi_{10} U_3 + U_5) H^3 / 12
\end{aligned} \tag{2}$$

The thermal force and moment vectors also involve the thermal coefficients, α_1 and α_2 :

$$\begin{aligned}
\begin{Bmatrix} N_x^{\text{Thermal}} \\ N_y^{\text{Thermal}} \\ N_{xy}^{\text{Thermal}} \end{Bmatrix} &= \frac{H}{2} \begin{Bmatrix} (U_1 + U_4)(\alpha_1 + \alpha_2) + U_2(\alpha_1 - \alpha_2) + \xi_1[U_2(\alpha_1 + \alpha_2) + (U_1 + 2U_3 - U_4)(\alpha_1 - \alpha_2)] \\ (U_1 + U_4)(\alpha_1 + \alpha_2) + U_2(\alpha_1 - \alpha_2) - \xi_1[U_2(\alpha_1 + \alpha_2) + (U_1 + 2U_3 - U_4)(\alpha_1 - \alpha_2)] \\ \xi_3[U_2(\alpha_1 + \alpha_2) + (U_1 + 2U_3 - U_4)(\alpha_1 - \alpha_2)] \end{Bmatrix} \Delta T \\
\begin{Bmatrix} M_x^{\text{Thermal}} \\ M_y^{\text{Thermal}} \\ M_{xy}^{\text{Thermal}} \end{Bmatrix} &= \frac{H^2}{8} \begin{Bmatrix} \xi_5[U_2(\alpha_1 + \alpha_2) + (U_1 + 2U_2 - U_4)(\alpha_1 - \alpha_2)] \\ -\xi_5[U_2(\alpha_1 + \alpha_2) + (U_1 + 2U_3 - U_4)(\alpha_1 - \alpha_2)] \\ \xi_7[U_2(\alpha_1 + \alpha_2) + (U_1 + 2U_2 - U_4)(\alpha_1 - \alpha_2)] \end{Bmatrix} \Delta T
\end{aligned} \tag{3}$$

where the laminate invariants, U_i , are defined as:

$$\begin{aligned}
U_1 &= \frac{(3Q_{11} + 3Q_{22} + 2Q_{12} + 4Q_{66})}{8} & U_2 &= \frac{(Q_{11} - Q_{22})}{2} & U_3 &= \frac{(Q_{11} + Q_{22} - 2Q_{12} - 4Q_{66})}{8} \\
U_4 &= \frac{(Q_{11} + Q_{22} + 6Q_{12} - 4Q_{66})}{8} & U_5 &= \frac{(Q_{11} + Q_{22} - 2Q_{12} + 4Q_{66})}{8}
\end{aligned} \tag{4}$$

and lamination parameters, ξ_j , are defined in condensed form as:

$$\xi_1, \xi_2, \xi_3, \xi_4 = \frac{1}{n} \sum_{k=1}^n (z_k - z_{k-1}) (\cos 2\theta_k, \cos 4\theta_k, \sin 2\theta_k, \sin 4\theta_k)$$

$$\xi_5, \xi_6, \xi_7, \xi_8 = \frac{2}{n^2} \sum_{k=1}^n (z_k^2 - z_{k-1}^2) (\cos 2\theta_k, \cos 4\theta_k, \sin 2\theta_k, \sin 4\theta_k) \quad (5)$$

$$\xi_9, \xi_{10}, \xi_{11}, \xi_{12} = \frac{4}{n^3} \sum_{k=1}^n (z_k^3 - z_{k-1}^3) (\cos 2\theta_k, \cos 4\theta_k, \sin 2\theta_k, \sin 4\theta_k)$$

with the implied convention that each comma separated lamination parameter on the left-hand side of the equation relates to the corresponding trigonometric term on the right-hand side.

Finally, the reduced stiffness terms, Q_{ij} , are calculated from the engineering properties:

$$Q_{11} = E_1 / (1 - \nu_{12}\nu_{21}), \quad Q_{12} = \nu_{12}E_2 / (1 - \nu_{12}\nu_{21}), \quad Q_{22} = E_2 / (1 - \nu_{12}\nu_{21}), \quad Q_{66} = G_{12} \quad (6)$$

Due to the balanced nature of a single layer of plain weave, i.e., equal fibre volume fractions in the 0 and 90° directions, see Fig. 1, the warp and weft directions are indistinguishable, thus justifying the equal modulus ($E_1 = E_2$) condition assumed.

Hence, standard ply angle orientations, 0, 90 and $\pm 45^\circ$, simplify to 0 and 45°; since the orthogonal counterparts, 90 and -45° , possess exactly the same properties, respectively.

In addition, the laminate invariant $U_2 = 0$, since $Q_{11} = Q_{22}$ follows directly from the equal modulus assumption. The thermal coefficients $\alpha_1 = \alpha_2 = \alpha_{\text{Iso}}$ follow from the same physical reasoning, and are also readily demonstrated from α_{Iso} for the equivalent isotropic laminate and the reduced form for balanced plain weave, i.e.:

$$\alpha_{\text{iso}} = \frac{\alpha_1 + \alpha_2}{2} + \frac{(\alpha_1 - \alpha_2)U_2}{2(U_1 + 2U_4)} \quad (7)$$

$$\alpha_{\text{iso}} = \frac{\alpha_1 + \alpha_2}{2}$$

Note that mechanical isotropy also leads to thermal isotropy but the reverse is not necessarily true, i.e., thermal isotropy does not guarantee mechanical isotropy.

As a result of these simplifications, the elements of the **ABD** matrix in Eq. (1) simplify compared to those for laminates containing layers of unidirectional material, giving:

$$\begin{aligned}
A_{11} &= (U_1 + \xi_2 U_3) H & B_{11} &= (\xi_6 U_3) H^2 / 4 & D_{11} &= (U_1 + \xi_{10} U_3) H^3 / 12 \\
A_{12} = A_{21} &= (-\xi_2 U_3 + U_4) H & B_{12} = B_{21} &= (-\xi_6 U_3) H^2 / 4 & D_{12} = D_{21} &= (U_4 - \xi_{10} U_3) H^3 / 12 \\
A_{16} = A_{61} &= (\xi_4 U_3) H & B_{16} = B_{61} &= (\xi_8 U_3) H^2 / 4 & D_{16} = D_{61} &= (\xi_{12} U_3) H^3 / 12 \\
A_{22} &= (U_1 + \xi_2 U_3) H & B_{22} &= (\xi_6 U_3) H^2 / 4 & D_{22} &= (U_1 + \xi_{10} U_3) H^3 / 12 \\
A_{26} = A_{62} &= (-\xi_4 U_3) H & B_{26} = B_{62} &= (-\xi_8 U_3) H^2 / 4 & D_{26} = D_{62} &= (-\xi_{12} U_3) H^3 / 12 \\
A_{66} &= (-\xi_2 U_3 + U_5) H & B_{66} &= (-\xi_6 U_3) H^2 / 4 & D_{66} &= (-\xi_{10} U_3 + U_5) H^3 / 12
\end{aligned} \tag{8}$$

and for the force and moment vectors:

$$\begin{Bmatrix} N_x^{\text{Thermal}} \\ N_y^{\text{Thermal}} \\ N_{xy}^{\text{Thermal}} \end{Bmatrix} = H \begin{Bmatrix} (U_1 + U_4) \alpha_{\text{iso}} \\ (U_1 + U_4) \alpha_{\text{iso}} \\ 0 \end{Bmatrix} \Delta T \tag{9}$$

$$\begin{Bmatrix} M_x^{\text{Thermal}} \\ M_y^{\text{Thermal}} \\ M_{xy}^{\text{Thermal}} \end{Bmatrix} = \begin{Bmatrix} 0 \\ 0 \\ 0 \end{Bmatrix}$$

involving a reduced set of laminate invariants, U_i :

$$\begin{aligned}
U_1 &= \frac{(6Q_{11} + 2Q_{12} + 4Q_{66})}{8} & U_3 &= \frac{(2Q_{11} - 2Q_{12} - 4Q_{66})}{8} \\
U_4 &= \frac{(2Q_{11} + 6Q_{12} - 4Q_{66})}{8} & U_5 &= \frac{(2Q_{11} - 2Q_{12} + 4Q_{66})}{8}
\end{aligned} \tag{10}$$

and consequently a reduced set of lamination parameter constraints:

$$\xi_2, \xi_4 = \frac{1}{n} \sum_{k=1}^n (z_k - z_{k-1}) (\cos 4\theta_k, \sin 4\theta_k)$$

$$\xi_6, \xi_8 = \frac{2}{n^2} \sum_{k=1}^n (z_k^2 - z_{k-1}^2) (\cos 4\theta_k, \sin 4\theta_k) \quad (11)$$

$$\xi_{10}, \xi_{12} = \frac{4}{n^3} \sum_{k=1}^n (z_k^3 - z_{k-1}^3) (\cos 4\theta_k, \sin 4\theta_k)$$

Additionally, for axis-aligned laminates, i.e. where the principal material axis is coincident with the system or structural axis, the lamination parameters ξ_4 , ξ_8 , and ξ_{12} are zero for standard ply angle orientations (0 and 45°), and correspond to $A_{16} = A_{26} = 0$, $B_{16} = B_{26} = 0$ and $D_{16} = D_{26} = 0$, respectively.

Different forms of the **ABD** matrix arise from off-axis alignment, β , of the principal material axis with respect to the system or structural axis for unidirection and plain weave materials. The square symmetric forms giving rise to HTCS laminates are summarized in Tables 2 and 3.

The square symmetric form of each of these matrices, which is common to all balanced plain weave laminates, implies that the general form remains unchanged, but because the magnitude of the terms vary sinusoidally, specific off-axis rotations, β , render certain coupling terms zero. This unique feature can therefore be exploited to tailor the mechanical coupling properties, without affecting the immunity to thermal warping distortions.

Table 2 demonstrates these relationships for the extensional [**A**] and bending [**D**] stiffness properties, which are uncoupled when the principal material axes are orthogonal to the system or structural axes, but are coupled in Extension-Shearing (*E-S*)

1 and Bending-Twisting (*B-T*), respectively, for all other axis alignments. Table 3
2 demonstrates the more complicated relationships for the coupling [**B**] matrix. For
3 instance Extension-Twisting and Shearing-Bending (*E-T-S-B*) coupling, presented in the
4 middle column of Table 3, is of particular practical interest for rotor blade design;
5 Extension-Twisting coupling is also the response most easily validated experimentally
6 [20]. Tables 2 and 3 also provide a comparison between response based labelling and
7 the ESDU [19] subscript notation, as well as the associated lamination parameter
8 constraints described below Eq. (11).
9

10 Note that the *cause-effect* relationships, corresponding to the form of the stiffness
11 matrix, are reversible and have complete duplicity with respect to the compliance matrix
12 for the coupled laminates, but only if the extensional [**A**] and the bending [**D**] matrix are
13 uncoupled (Simple), see Table 4. Extension-Shearing and/or Bending-Twisting
14 coupling give rise to secondary couplings, which are revealed by inspection of the
15 compliance matrix. Note that whilst these secondary couplings are directly influenced
16 by the specific form of each of the three stiffness sub-matrices, [**A**], [**B**], and [**D**], square
17 symmetry is always preserved. A comparison of the *cause-effect* relationship for the *E-*
18 *T-S-B;B-T* coupled laminate with respect to the form of the compliance matrix in Table
19 4 reveals that an applied mechanical force resultant N_x , gives rise to twisting curvatures
20 as well as extensional strains as a result of the Extension-Twisting (*E-T*) coupling
21 behaviour, but also to secondary bending curvatures, which arise from the twisting
22 curvatures as a result of Bending-Twisting (*B-T*) coupling behaviour, i.e., $b_{11} \neq 0$.
23 Finally, the secondary bending curvatures lead to tertiary shearing strains through
24 Shearing-Bending (*S-B*) coupling behaviour, i.e., $a_{16} \neq 0$. Only through calculation are
25 the relative magnitudes of the secondary couplings revealed. However, this scenario
26
27
28
29
30
31
32
33
34
35
36
37
38
39
40
41
42
43
44
45
46
47
48
49
50
51
52
53
54
55
56
57
58
59
60
61
62
63
64
65

1 serves to demonstrates the validity of the *cause-effect* relationships, based on the form
2
3 of the stiffness matrix, rather than compliance matrix, not only as a general descriptor of
4
5 the laminate coupling behaviour, but also for assessing the presence of any secondary
6
7 couplings without the requirement for matrix inversion.
8
9

10
11 Isotropy in the thermal force vector of Eq. (8), a zero thermal moment vector, and
12
13 square symmetry in the extensional $[A]$ and coupling $[B]$ stiffness matrices are the
14
15 necessary conditions for HTCS laminates [10,11]. The equal principal strains that result
16
17 from the isotropic thermal force vector imply that the Mohr's circle for strain
18
19 transformations degenerates to a point (in the same way that Mohr's circle for stress
20
21 degenerates to a point under a hydrostatic stress state), hence thermal strains are
22
23 identical in all directions and therefore plies of any orientation may be laminated
24
25 together without warping following post-cure cool-down.
26
27
28
29
30

31 It is worth noting that the bending $[D]$ stiffness matrix is square symmetric for all
32
33 balanced plain weave laminates, but this is not a necessary condition for HTCS
34
35 laminates, as demonstrate elsewhere [10] for laminates consisting of unidirectional
36
37 material.
38
39

40
41 In fact only two parent classes exist for laminates with balanced plain weave and
42
43 standard ply angle orientations: the Simple ($A_S B_0 D_S$) laminate and; the Extension-
44
45 Bending and Shearing-Twisting (*E-B-S-T*) coupled ($A_S B_S D_S$) laminate. All other
46
47 mechanical coupling responses arise from off-axis orientation, β , of the principal
48
49 material axes of these parent laminates, with respect to the system or structural axes.
50
51
52
53
54
55
56
57
58
59
60
61
62
63
64
65

3. Results and Discussion

3.1 Uncoupled Laminates with Balanced Plain Weave

The most commonly adopted method for achieving fully uncoupled laminates is through the use of balanced and symmetric construction. However, non-symmetric laminate configurations are now known to dominate the design space of Simple (uncoupled) laminates. The Simple ($\mathbf{A}_S\mathbf{B}_0\mathbf{D}_S$) laminate is identified from solutions with lamination parameters:

$$\xi_6 = \xi_8 = 0 \quad (12)$$

where $\xi_8 = 0$ due to the standard ply angle orientations adopted.

A sub-group of fully isotropic ($\mathbf{A}_I\mathbf{B}_0\mathbf{D}_I$) laminates also exist from within the Simple ($\mathbf{A}_S\mathbf{B}_0\mathbf{D}_S$) laminate class, and can be identified through the additional lamination parameter constraints:

$$\xi_2 = \xi_4 = \xi_{10} = \xi_{12} = 0 \quad (13)$$

from which Eq. (8) reveals that the extensional [\mathbf{A}] and bending [\mathbf{D}] stiffness matrices depend solely on the laminate invariants, U_i , i.e. the material properties. Here, the extensional stiffnesses:

$$A_{11} = A_{22} \text{ and } A_{66} = (A_{11} - A_{12})/2 \quad (14)$$

are concomitant with the bending stiffnesses, i.e.:

$$D_{ij} = A_{ij}H^2/12 \quad (15)$$

which together correspond to the fully isotropic condition.

1 The polar plots of Fig. 2 demonstrate the lamination parameter and extensional stiffness
2 variations for a single layer of balanced plain weave fabric with off-axis orientation $0^\circ \leq$
3 $\beta \leq 360^\circ$. The more common form, demonstrating effective moduli, is also presented.
4
5
6 Note that Eq. (15) applies in the single layer case, hence $\xi_{10} = \xi_2$ and $\xi_{12} = \xi_4$.
7
8
9

10
11 Vincenti *et al.* [21] adopted the polar method, developed by Verchery [22], to
12 investigate specific properties of uncoupled balanced plain weave laminates. Some
13 interesting solutions were given demonstrating that the square symmetric concomitant
14 properties in extension and bending can also be tailored, through the use of non-
15 standard ply angle orientations, so that the alignment of principal extensional stiffness is
16 different to the principal bending stiffness. By contrast, Grediac [23] found
17 approximate solutions with extensional isotropy and fully isotropic properties, for
18 laminates with up to 11 plies, by solving the lamination parameter constraints using an
19 optimisation strategy with free form ply angle orientations. The single, exact solution,
20 found for an 8-ply fully isotropic laminate, with standard ply angle orientations, is
21 reconfirmed in this article together with exact solutions for higher ply number
22 groupings.
23
24
25
26
27
28
29
30
31
32
33
34
35
36
37
38
39
40

41 The number of solutions for Simple ($\mathbf{A}_S\mathbf{B}_0\mathbf{D}_S$) laminates is presented in Table 5 for each
42 ply number grouping with up to 21 plies. These Simple laminates also contain sub-
43 groups with quasi-homogeneous ($\mathbf{A}_S\mathbf{B}_0\mathbf{D}_S$) and fully isotropic ($\mathbf{A}_I\mathbf{B}_0\mathbf{D}_I$) properties, both
44 satisfying Eq. (15), and extensionally isotropic ($\mathbf{A}_I\mathbf{B}_0\mathbf{D}_S$) properties, all of which are
45 quantified in Table 5. Where single quasi-homogeneous solutions are reported for
46 particular ply number groupings, the form of the stacking sequence is represented by
47 $[\alpha]_{rT}$, where the number of repetitions, r , corresponds to the number of plies, n ; all share
48 the same non-dimensional properties as the single ply, shown in Fig. 2.
49
50
51
52
53
54
55
56
57
58
59
60
61
62
63
64
65

1 An abridged listing of stacking sequences for Simple ($A_S B_0 D_S$) laminates with up to 21
2 plies is presented in the appendix (Table A2); these are ordered by increasing
3
4
5
6 compression buckling strength, corresponding to the infinitely long plate with simply
7
8 supported edges, for which the closed form solution of Eq. (16) is applicable. The
9
10 complete list of stacking sequences for fully isotropic laminates with up to 21 plies is
11
12 presented in Table 6.
13
14
15

16 **3.2 Coupled Laminates with Balanced Plain Weave**

17
18
19 The coupled parent ($A_S B_S D_S$) laminate class possesses Extension-Bending and
20
21 Shearing-Twisting ($E-B-S-T$) coupling, which corresponds to the lamination parameter
22
23 constraint:
24
25

$$26 \xi_6 \neq 0 \quad (16)$$

27
28
29 Additional coupling characteristics can be obtained from this parent laminate class by
30
31 applying off-axis material alignment, β .
32
33
34
35

36
37 Note that the HTCS condition, present in a single layer of balanced plain weave
38
39 material is retained for general off-axis material alignment, β . This extends to all plain
40
41 weave laminates, irrespective of the number of plies in the laminate or the laminate
42
43 stacking sequence. By contrast, fibre misalignment errors in the stacking sequences for
44
45 HTCS laminates with unidirectional material, or unbalanced plain weave, will
46
47 inevitably give rise to some degree of thermal warping. Additionally, HTCS laminates
48
49 with unidirectional material are achievable only for certain ply number groupings when
50
51 standard ply angle orientations are adopted [10], i.e., with 8, 12, 16 and 20 plies, etc. It
52
53
54
55
56 has however recently been shown [24] that HTCS solutions can be achieved in all ply
57
58
59
60
61
62
63
64
65

1 number groupings with 10 plies and above if non-standard ply orientations are adopted,
2
3 i.e., $\theta = 0, 90$ and $\pm 60^\circ$.
4
5

6 Seven classes of coupled laminate can be produced from balanced plain weave material.
7
8 All are derived from the single parent ($\mathbf{A}_S\mathbf{B}_S\mathbf{D}_S$) laminate class, through the off-axis
9 alignments detailed in Tables 2 and 3. The 6 derivatives are summarized in Table 7. In
10 addition, a sub-group of these coupled laminates have been discovered with both
11 extensional and bending stiffness isotropy; solutions which also possess compliance
12 isotropy. Illustrations in Table 7 represent unconstrained thermal contraction responses
13 that would typically result at room temperature, following a standard high temperature
14 curing process. They provide classical laminate theory predictions of the warping
15 behaviour that is avoided in balanced plain weave laminates, by virtue of their HTCS
16 properties, for all 7 classes of mechanical coupling. Note that the stacking sequences
17 given are representative samples from the minimum ply number grouping for each class
18 of coupled laminate; given as the parent laminate, with standard ply angle orientations,
19 prior to off-axis material alignment, β , where $\alpha = \beta + \pi/4$.
20
21
22
23
24
25
26
27
28
29
30
31
32
33
34
35
36
37
38

39 The number of solutions in each of the 7 coupled laminate classes are listed in Table 8.
40
41 The second column of the table represents the number of Extension-Bending and
42 Shearing-Twisting (E-B-S-T) parent ($\mathbf{A}_S\mathbf{B}_S\mathbf{D}_S$) laminate solutions for each ply number
43 grouping, n . Subsequent columns demonstrate the number of solutions in each coupled
44 laminate derivative arising from a specific off-axis orientation, β . The results reveal
45 that the two parent solutions for the 2-ply laminate ($n = 2$) give rise to either the $\mathbf{A}_S\mathbf{B}_T\mathbf{D}_S$
46 or the $\mathbf{A}_S\mathbf{B}_F\mathbf{D}_S$ coupled laminate classes following off-axis rotation. Both solutions are
47 fully isotropic in Extension [\mathbf{A}] and Bending [\mathbf{D}] and therefore an off-axis rotation
48 changes only the Coupling [\mathbf{B}] matrix properties. For instance, off-axis material
49
50
51
52
53
54
55
56
57
58
59
60
61
62
63
64
65

1 alignment, $\beta = \pi/8$, applied to the 2-ply $[\alpha/\beta]_T$ parent laminate (i.e., the configuration
 2 represented in the first column of Table 7,) gives rise to $E-T-S-B$ coupling (or $B-S-T-E$
 3 since each *cause-effect* pairing is reversible), which corresponds to $\xi_6 = 0$ and the
 4 associated form of the coupling stiffness matrix in Table 3. Bending-Extension and
 5 Twisting-Shearing or $B-E-T-S$ coupling exists for all other off-axis alignments.
 6
 7
 8
 9
 10

11 The polar plots of Fig. 3 best illustrate the sinusoidal relationship of lamination
 12 parameters with off-axis material alignment. Extension-Twisting and Shearing-Bending
 13 or $E-T-S-B$ coupled ($\mathbf{A}_S\mathbf{B}_T\mathbf{D}_S$) laminates are shown in Table 8 to exist only for even ply
 14 number groupings. An abridged listing of laminate stacking sequences is presented in
 15 the appendix (Table A3), in order of increasing magnitude of the Extension-Twisting
 16 coupling magnitude, i.e., increasing ξ_8 or \mathbf{B}_{16} . The polar plots demonstrate that the
 17 lamination parameters $\xi_2 = \xi_4 = 0$ and $\xi_{10} = \xi_{12} = 0$ for all axis alignments, signifying
 18 isotropic properties in extension and bending, respectively.
 19
 20
 21
 22
 23
 24
 25
 26
 27
 28
 29
 30
 31
 32

33 By contrast, Table 8 reveals that the parent solutions for the 3-ply laminates ($n = 3$) give
 34 rise to either the $\mathbf{A}_F\mathbf{B}_T\mathbf{D}_F$ or the $\mathbf{A}_F\mathbf{B}_F\mathbf{D}_F$ coupled laminate classes. The polar plots of
 35 Fig. 4 illustrate the variation in lamination parameters with off-axis alignment for the
 36 stacking sequence $[\alpha/\beta_2]_T$, which corresponds to the example stacking sequence in the
 37 third column of Table 7. Here, Extension-Shearing coupling is present ($\xi_4 \neq 0$) for all
 38 axis orientations, except those corresponding to orthogonal axes, i.e., $\beta = m\pi/4$ ($m = 0,$
 39 $1, 2, \dots$), the Coupling $[\mathbf{B}]$ stiffness matrix properties are similar to the previous 2-ply
 40 example, but with a reduced magnitude, and the bending stiffness properties
 41 approximate isotropic behaviour but are in fact numerically zero only for $\beta = m\pi/4$ ($m =$
 42 $0, 1, 2, \dots$).
 43
 44
 45
 46
 47
 48
 49
 50
 51
 52
 53
 54
 55
 56
 57
 58
 59
 60
 61
 62
 63
 64
 65

1 Finally, the 28 solutions for 6-ply laminates ($n = 6$), presented in Table 8 result in all six
 2
 3 mechanically coupled classes as a result of off-axis orientation, β . Figure 5 illustrates
 4
 5 the polar plots of lamination parameter relationships for the 6-ply stacking sequence
 6
 7 $[\alpha/\beta/\alpha_2/\beta_2]_T$. In this case the lamination parameters $\xi_2 = \xi_4 = 0$ for all axis alignments,
 8
 9 indicating that this laminate possesses isotropic extensional $[\mathbf{A}]$ stiffness properties.
 10
 11 However, this is not a true isotropy condition since it not reflected in the compliance
 12
 13 relationship, where the isotropy is lost as a result of the influence of Bending-Twisting
 14
 15 coupling through the Coupling $[\mathbf{B}]$ matrix. Once again the Coupling $[\mathbf{B}]$ stiffness
 16
 17 matrix properties are similar to the previous examples, albeit with different magnitude.
 18
 19 Bending-Twisting coupling is present at all off-axis orientations, since $\xi_{12} = 0$ only for β
 20
 21 $= m\pi/4$ ($m = 0, 1, 2, \dots$). This example represents the $\mathbf{A}_S\mathbf{B}_T\mathbf{D}_F$ and $\mathbf{A}_S\mathbf{B}_F\mathbf{D}_F$ laminate
 22
 23 classes in Table 7, depending on the specific off-axis orientation, β .
 24
 25
 26
 27
 28
 29
 30

31 **4. Laminate Design**

32
 33
 34
 35 This section presents two worked examples, the first of which is a comparison of
 36
 37 unidirectional and balanced plain weave laminates for a rotor blade application in which
 38
 39 maximum twist, through mechanical extension-twisting coupling, is required under a
 40
 41 given centrifugal loading condition. The stacking sequences chosen have the highest
 42
 43 coupling magnitude achievable using standard ply angle orientations, i.e. 0, 90 and
 44
 45 $\pm 45^\circ$. It should be noted however that whilst standard ply orientations were chosen to
 46
 47 satisfy manufacturing constraints, the laminates are assumed to be loaded off-axis, in
 48
 49 order to induce extension-twisting coupling. The stacking sequence chosen to represent
 50
 51 the balanced plain weave laminate, $[\alpha_2/\beta_2]_T$, therefore corresponds to $[67.5_2/22.5_2]_T$ in
 52
 53 accordance with the design rules of Table 3, i.e., an off-axis orientation, $\beta = \pi/8$. The
 54
 55
 56
 57
 58
 59
 60
 61
 62
 63
 64
 65

1 competing unidirectional laminate of equal thickness, whose stacking sequence has
 2
 3 been derived independently by others [1,9,10], corresponds to [-22.5/67.5₂/-22.5/22.5/
 4
 5 67.5₂/22.5]_T, following off-axis orientation.
 6
 7

8
 9 The reduced stiffnesses are readily calculated from the material properties of Table 1
 10 using Eq. (6), giving $Q_{11} = Q_{22} = 90,226$, $Q_{12} = 4,511$ and $Q_{66} = 5,000$ (N/mm²) for
 11 balanced plain weave material. The laminate invariants $U_1 = 71,297$, $U_3 = 18,929$, $U_4 =$
 12 $23,440$ and $U_5 = 23,929$ (N/mm²) follow from Eq. (10) and the only non-zero
 13 lamination parameter, obtained from Eq. (11), is $\xi_8 = 1$. The elements of the **ABD**
 14 matrix then follow from Eq. (8), giving:
 15
 16
 17
 18
 19
 20
 21
 22
 23

$$\begin{bmatrix}
 104,379 & 34,316 & 0 & 0 & 0 & 10,142 \\
 34,316 & 104,379 & 0 & 0 & 0 & -10,142 \\
 0 & 0 & 35,031 & 10,142 & -10,142 & 0 \\
 0 & 0 & 10,142 & 18,643 & 6,129 & 0 \\
 0 & 0 & -10,142 & 6,129 & 18,643 & 0 \\
 10,142 & -10,142 & 0 & 0 & 0 & 6,257
 \end{bmatrix} \quad (17)$$

24
 25
 26
 27
 28
 29
 30
 31
 32
 33
 34
 35
 36 For the unidirectional material comparator, the reduced stiffnesses also follow from
 37 Table 1, using Eq. (6), but now the laminate invariants follow from Eq. (4), the two
 38 non-zero lamination parameters, $\xi_8 = 1$ and $\xi_9 = 0.133$, follow from Eq. (5) and the
 39 elements of the **ABD** matrix follow from Eq. (2), giving:
 40
 41
 42
 43
 44
 45

$$\begin{bmatrix}
 102,765 & 32,342 & 0 & 0 & 0 & 10,530 \\
 32,342 & 102,765 & 0 & 0 & 0 & -10,530 \\
 0 & 0 & 35,212 & 10,530 & -10,530 & 0 \\
 0 & 0 & 10,530 & 21,156 & 5,776 & 0 \\
 0 & 0 & -10,530 & 5,776 & 21,156 & 0 \\
 10,530 & -10,530 & 0 & 0 & 0 & 6,289
 \end{bmatrix} \quad (18)$$

The twisting magnitude of the two laminates is assessed using a geometrically non-linear finite element model [25], validated against experimental results for laminates with similar mechanical coupling behaviour. The specimen (25mm × 180mm) was modelled with thin shell (S8R5) elements; 5 elements across the width and 38 elements along the length of the specimen were sufficient to provide good convergence; the boundary conditions, matching previous experiments, were applied via rigid body elements to a reference node at which the load was applied and axial extension and rotation measured.

Figure 6 shows the axial load vs. twist-rate for the two laminate comparators, where the twisting magnitude of each laminate is assessed up to an axial load corresponding to the predicted first ply failure load, using the Tsai-Wu failure criterion:

$$F_1\sigma_1 + F_2\sigma_2 + F_{11}\sigma_1^2 + F_{22}\sigma_2^2 + F_{66}\tau_{12}^2 - (F_{11}F_{22})^{1/2} \sigma_1\sigma_2 = 1$$

where,

$$F_1 = (1/\sigma_1^T + 1/\sigma_1^C), \quad (19)$$

$$F_2 = (1/\sigma_2^T + 1/\sigma_2^C)$$

$$F_{11} = -1/\sigma_1^T\sigma_1^C,$$

$$F_{22} = -1/\sigma_2^T\sigma_2^C,$$

$$F_{66} = (1/\tau_{12}^F)^2$$

using the material strength properties given in Table 1.

The predicted failure loads under uniaxial tension, derived using the inverse of Eq. (1), see Table 4, are 10.72 kN and 9.42 kN for the unidirectional and balanced plain weave materials, respectively. However, the finite element analyses predict failure loads of 11.45 kN and 10.10 kN, due to the applied boundary conditions, which simulate the tension grips of a tension-torsion test machine.

This example demonstrates that the design constraint of square symmetry in the **A** and **B** stiffness matrices, necessary to avoid thermal warping distortion in coupled laminates, has the effect of reducing the advantages of unidirectional material over balanced plain weave material.

A second example compares the compression buckling strength for unidirectional and balanced plain weave, using the same stacking sequences. Note that the elements of the **ABD** matrix in Eqs (17) and (18) must first be recalculated using the compressive moduli of Table 1. The Tsai-Wu failure criterion failure loads under uniaxial compression, derived using the inverse of Eq. (1), are now 12.83 kN and 8.76 kN, respectively.

The buckling strength of Extension-Twisting (and Shearing-Bending) coupled laminates can be calculated from a closed form buckling solution:

$$N_x = (a/m\pi)^2 \{ T_{33} + (2T_{12}T_{23}T_{13} - T_{22}T_{13}^2 - T_{11}T_{23}^2) / (T_{11}T_{22} - T_{12}^2) \}$$

with

$$\begin{aligned} T_{11} &= A_{11}(m\pi/a)^2 + A_{66}(n\pi/b)^2 \\ T_{12} &= (A_{12} + A_{66})(m\pi/a)(n\pi/b) \\ T_{13} &= -(3B_{16}(m\pi/a)^2 + B_{26}(n\pi/b)^2)(n\pi/b) \\ T_{22} &= A_{22}(n\pi/b)^2 + A_{66}(m\pi/a)^2 \\ T_{23} &= -(B_{16}(m\pi/a)^2 + 3B_{26}(n\pi/b)^2)(m\pi/a) \\ T_{33} &= D_{11}(m\pi/a)^4 + 2(D_{12} + 2D_{66})(m\pi/a)^2(n\pi/b)^2 + D_{22}(n\pi/b)^4 \end{aligned} \quad (20)$$

where, for the infinitely long case, m is a non-integer value, corresponding to the number of buckling half-waves along the plate length, a , or plate width, b , when $a = b$ is assumed.

Following minimisation of N_x , with respect to m and n , the buckling load can be expressed in non-dimensional form:

$$k_x = (N_x b^2) / (\pi^2 D_{\text{Iso}}) \quad (21)$$

where D_{Iso} is calculated from the laminate invariant, U_1 , and laminate thickness, H :

$$D_{\text{Iso}} = U_1 H^3 / 12 \quad (22)$$

This permits like-with-like comparison of laminates with any number of plies, n , and is the procedure adopted for generating k_x in Tables A2 and A3, since Eq. (20) degenerates to the closed form solution for orthotropic laminates when $B_{ij} = 0$. Note that due to the square symmetric form of the **A**, **B** and **D** matrices in all balanced plain weave laminates, $m = n = 1$ in Eq. (20), which corresponds to a buckling half-wavelength $\lambda = b$.

Equation (20) is often associated with anti-symmetric angle-ply laminates [26,27], but the non-symmetric stacking sequences presented in Table A3 demonstrate that these conditions are not a requirement. Buckling factors, $k_x = 3.04$ and 3.40 , are readily calculated for the comparator laminates with unidirectional and balanced plain weave materials, respectively. A lower k_x for the unidirectional laminate is expected, since it possesses the highest Extension-Twisting coupling magnitude of the two comparators; Extension-Twisting coupling has been shown [25] to be inversely proportional to the compression buckling strength. Table A3 demonstrates that for laminates with balanced plain weave the maximum coupling magnitude, $\xi_8 = 1$, gives a lower-bound buckling solution, $k_x = 3.40$, for stacking sequences of the form $[\alpha_{n/2}/\beta_{n/2}]_T$. By contrast, the upper-bound buckling solution tends toward $k_x = 4.00$ as lamination parameter, ξ_8 , approaches zero, i.e. the fully isotropic laminate. The stacking sequences in Table A3 possess lamination parameters $\xi_2 = \xi_4 = \xi_{10} = \xi_{12} = 0$ for all axis rotations, representing extensional and bending isotropy.

1 **5. Conclusions**
2
3

4 A definitive list of laminate stacking sequences has been derived for balanced plain
5
6 weave material with standard ply orientations used in industry.
7

8
9 Seven unique classes of coupled composite laminates have been demonstrated, and for
10
11 completeness, uncoupled laminates have been included together with an important sub-
12
13 group possessing fully isotropic properties.
14

15
16
17 Isotropy in bending and/or extensional stiffness has been found in both coupled as well
18
19 as uncoupled laminates.
20

21
22 The coupled classes arise from the judicious realignment of the principal material axis
23
24 of a so-called parent laminate class, which possesses Extension-Bending and Shearing-
25
26 Twisting: off-axis alignment, with respect to the structural or system axis, gives rise to
27
28 other distinct forms of coupling interaction.
29
30

31
32 All seven classes of coupled balanced plain weave laminate have immunity to thermal
33
34 warping distortions, which generally arise as a result of the high temperature curing
35
36 process. Such laminates therefore provide a robust manufacturing solution for
37
38 integrating complex mechanical coupling response, as an enabling technology, in future
39
40 smart materials and structures.
41
42
43
44
45
46
47
48
49
50
51
52
53
54
55
56
57
58
59
60
61
62
63
64
65

1
2 **References**
3

4 [1] Nixon, M.W., 1987. Extension-twist coupling of composite circular tubes with
5 application to tilt rotor blade design, 28th AIAA/ASME/ASCE/AHS/ASC Structures,
6 Structural Dynamics, and Materials, Monterey, United states, Paper No. AIAA-87-
7 0772.
8

9 [2] Winckler, S.J., 1985. Hygrothermally Curvature Stable Laminates with Tension-
10 Torsion Coupling. Journal of the American Helicopter Society, 30, 56-58.
11

12 [3] York, C.B., 2010. Unified approach to the characterization of coupled composite
13 laminates: Benchmark configurations and special cases. Journal of Aerospace
14 Engineering, 23, 219-242.
15

16 [4] Tsai, S.W., Hahn, H.T., 1980. Introduction To Composite Materials. Technomic
17 Publishing Co. Inc., Lancaster.
18

19 [5] Chen, H.P., 2003. Study of hygrothermal isotropic layup and hygrothermal
20 curvature-stable coupling composite laminates, 44th AIAA/ASME/ASCE/AHS/ASC
21 Structures, Structural Dynamics, and Materials Conference. American Inst. Aeronautics
22 and Astronautics Inc., Norfolk, VA, United States, 958-967.
23

24 [6] Cross, R.J., Haynes, R.A., Armanios, E.A., 2008. Families of Hygrothermally Stable
25 Asymmetric Laminated Composites. Journal of Composite Materials, 42, 697-716.
26

27 [7] Diaconu, C.G., Sekine, H., 2003. Flexural Characteristics and Layup Optimization
28 of Laminated Composite Plates Under Hygrothermal Conditions using Lamination
29 Parameters, Journal of Thermal Stresses, 26, 905-922.
30
31
32
33
34
35
36
37
38
39
40
41
42
43
44
45
46
47
48
49
50
51
52
53
54
55
56
57
58
59
60
61
62
63
64
65

- 1 [8] Diaconu, C.G., Sekine, H., 2004. Erratum on Flexural Characteristics and Layup
2 Optimization of Laminated Composite Plates Under Hygrothermal Conditions using
3 Lamination Parameters, *Journal of Thermal Stresses*, 27, 1213-1216.
4
5
6
7
8
9 [9] Weaver, P.M., 2005. Anisotropic laminates that resist warping during manufacture,
10 15th International Conference on Composite Materials, Durban, South Africa.
11
12
13
14 [10] York, C.B., 2011. Unified approach to the characterization of coupled composite
15 laminates Hygro-thermally curvature-stable configurations. *International Journal of*
16 *Structural Integrity*, 2, 406-436.
17
18
19
20
21
22 [11] Verchery, G., 2011. Design Rules for the Laminate Stiffness. *Mechanics of*
23 *Composite Materials*, 47, 47-58.
24
25
26
27 [12] Shamsudin, M.H., Rousseau, J., York, C.B., 2013. Warping Curvature Predictions
28 for Non-Symmetric Woven Cloth Laminates. Proc. 12th Deformation and Fracture of
29 Composites and 6th Structural Integrity and Multi-scale Modelling Conf., Cambridge,
30 England.
31
32
33
34
35
36
37 [13] Ishikawa, T., Chou, T.W., 1982. Stiffness and strength behaviour of woven fabric
38 composites. *Journal of Materials Science*, 17, 3211-3220.
39
40
41
42 [14] Naik, N.K., Shembekar, P.S., 1992. Elastic Behavior of Woven Fabric Composites:
43 I - Lamina Analysis. *Journal of Composite Materials*, 26, 2196-2225.
44
45
46
47 [15] Raju, I.S., Wang, J.T., 1994. Classical laminate theory models for woven fabric
48 composites. *Journal of Composites Technology and Research*, 16, 289-303.
49
50
51
52 [16] Naik, N.K., Shembekar, P.S., 1992. Elastic Behavior of Woven Fabric Composites:
53 III - Laminate Design. *Journal of Composite Materials*, 26, 2522-2541.
54
55
56
57
58
59
60
61
62
63
64
65

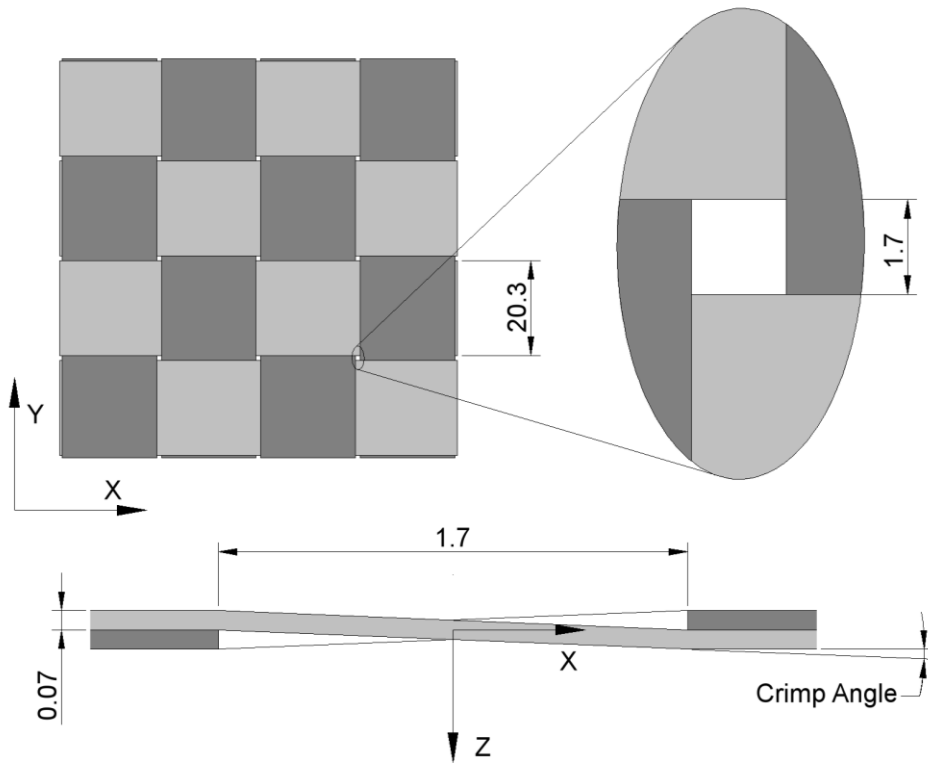
- 1 [17] Ishikawa, T., Matsushima, M., Hayashi, Y., Chou, T.W., 1985. Experimental
2 Confirmation of the Theory of Elastic Moduli of Fabric Composites. Journal of
3 Composite Materials, 19, 443-458.
4
5
6
7
8
9 [18] Jekabsons, N., Byström, J., 2002. On the effect of stacked fabric layers on the
10 stiffness of a woven composite. Composites Part B: Engineering, 33, 619-629.
11
12
13
14 [19] ESDU, 1994. Stiffnesses of laminated flat plates Engineering Science Data Unit
15 Item No. 94003, 1-28.
16
17
18
19 [20] Shamsudin, M.H., Roussea, J., Verchery, G., York, C.B., 2011. Experimental
20 Validation of the Mechanical Coupling Response for Hygro-Thermally Curvature-
21 Stable Laminated Composite Materials, 6th International Conference on Supply on the
22 Wings, Frankfurt, Germany.
23
24
25
26
27
28
29 [21] Vincenti, A., Verchery, G., Vannucci, P., 2001. Anisotropy and symmetry for
30 elastic properties of laminates reinforced by balanced fabrics. Composites Part A:
31 Applied Science and Manufacturing, 32, 1525-1532.
32
33
34
35
36
37 [22] Verchery, G., 1979. Les invariants d'ordre 4 du type de l'élasticité. Euromech
38 Colloquium 115, Villard-de-Lans, France, 93–104.
39
40
41
42 [23] Grediac, M., 2001. On the stiffness design of thin woven composites. Composite
43 Structures, 51, 245-255.
44
45
46
47 [24] York, C.B., 2013. Tapered hygro-thermally curvature-stable laminates with non-
48 standard ply orientations. Composites Part A: Applied Science and Manufacturing, 44,
49 140-148.
50
51
52
53
54
55
56
57
58
59
60
61
62
63
64
65

1 [25] Shamsudin, M.H., Chen, J., York, C.B., 2013. Bounds on the Compression
2 Buckling Strength of Hygro-Thermally Curvature-Stable Laminate with Extension-
3 Twisting Coupling. International Journal of Structural Integrity. In Press.
4
5

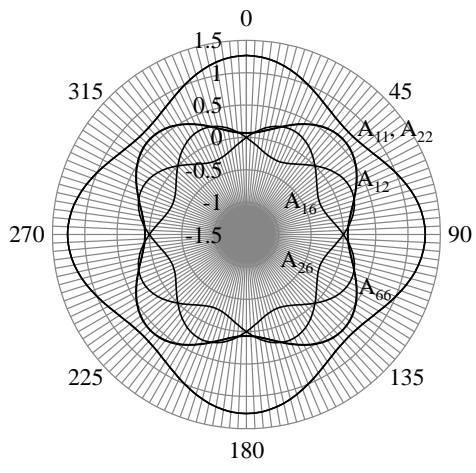
6
7
8 [26] Whitney, J.M., Leissa, A.W., 1969. Analysis of Heterogenous Anisotropic Plates.
9 Journal of Applied Mechanics, 36, 261-266.
10

11
12 [27] Jones, R.M., 1999. Mechanics of Composite Materials, 2nd Edition ed.
13 Blacksburg. Taylor & Francis, Inc., Virginia.
14
15
16
17
18
19
20
21
22
23
24
25
26
27
28
29
30
31
32
33
34
35
36
37
38
39
40
41
42
43
44
45
46
47
48
49
50
51
52
53
54
55
56
57
58
59
60
61
62
63
64
65

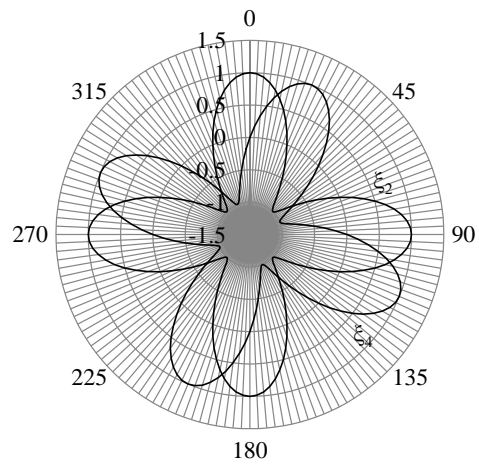
1 **Figures**



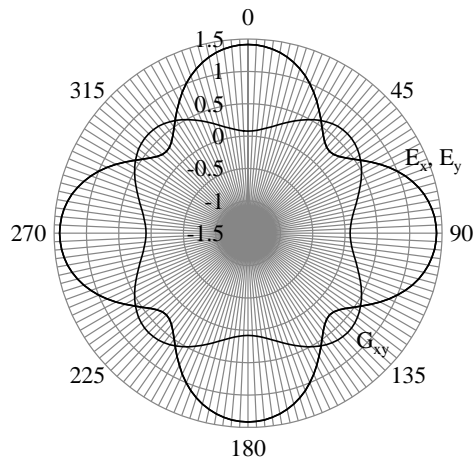
31 **Figure 1**



(a)

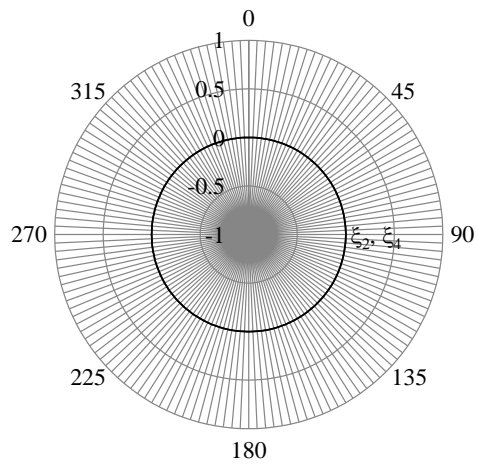


(b)

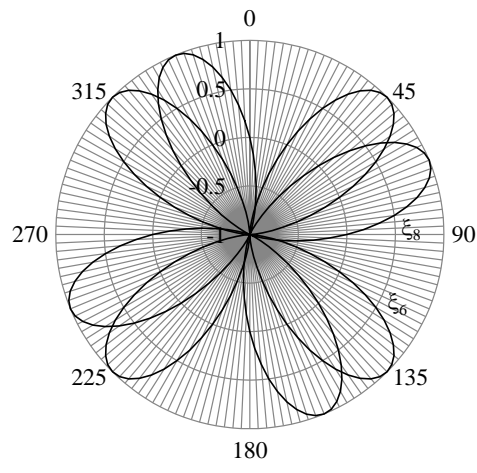


(c)

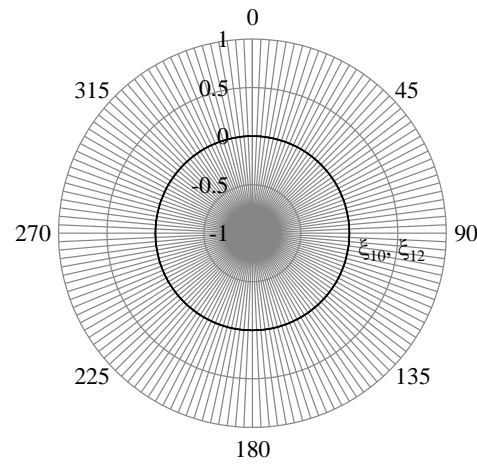
Figure 2



(a)

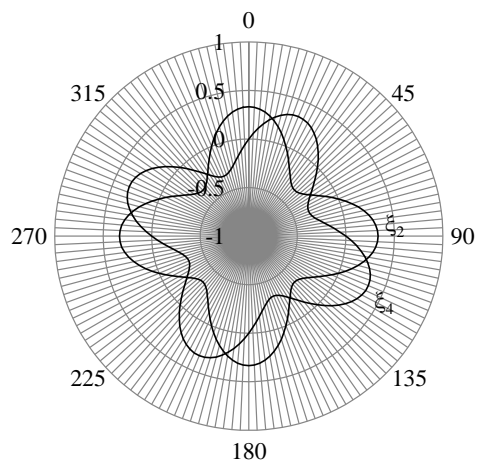


(b)

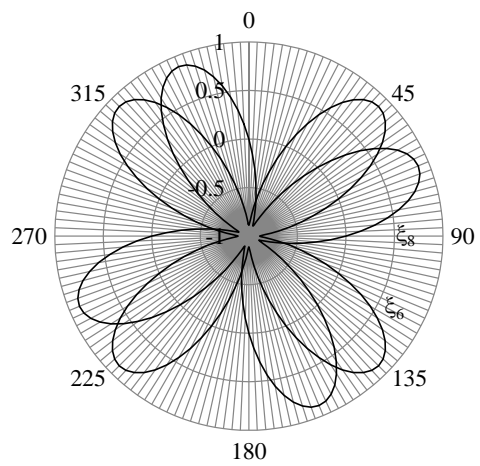


(c)

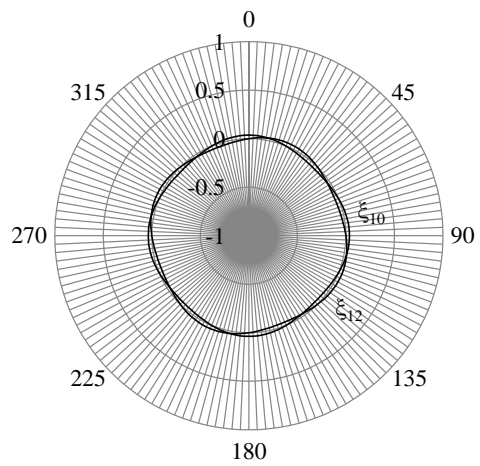
Figure 3



(a)



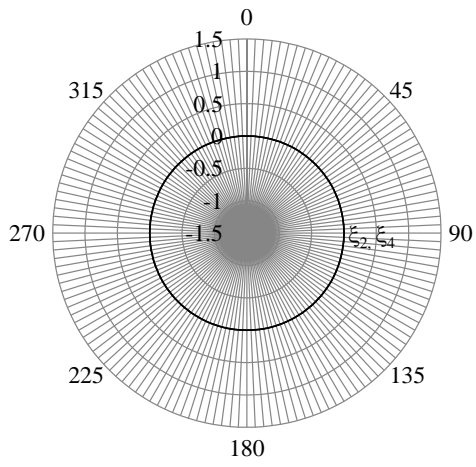
(b)



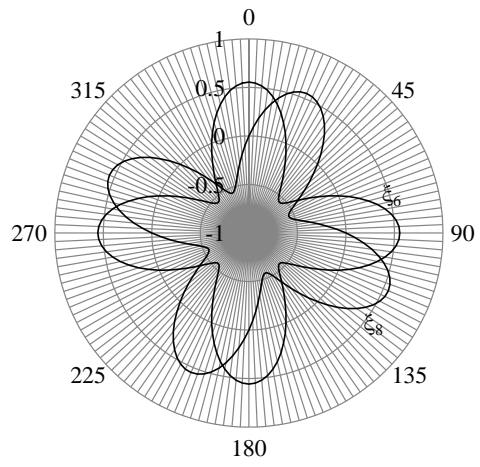
(c)

Figure 4

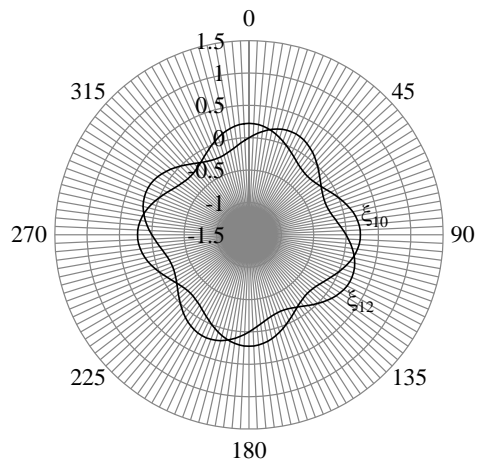
1
2
3
4
5
6
7
8
9
10
11
12
13
14
15
16
17
18
19
20
21
22
23
24
25
26
27
28
29
30
31
32
33
34
35
36
37
38
39
40
41
42
43
44
45
46
47
48
49
50
51
52
53
54
55
56
57
58
59
60
61
62
63
64
65



(a)



(b)



(c)

Figure 5

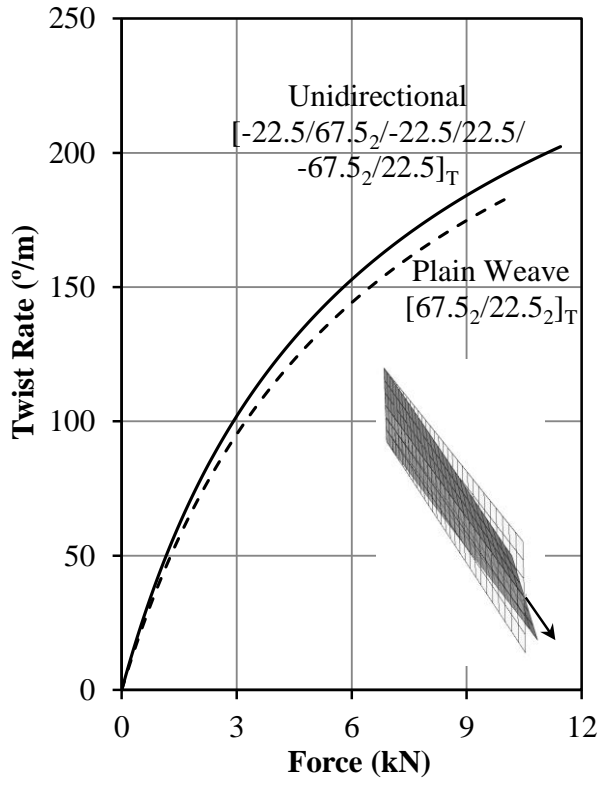


Figure 6.

1 **Figure Captions**
2
3
4

5 **Figure 1** - Balanced plain weave architecture, illustrating a plan view of a
6 representative volume element with exploded details. Dimensions provided are
7 representative of (TeXtreme[®]) spread tow fabric with 70µm tape thickness and 2.5°
8 crimp angle.
9
10
11
12
13
14
15
16
17
18

19 **Figure 2** - Polar plots for off-axis material alignment, $0^\circ \leq \beta \leq 360^\circ$, of: (a) extensional
20 stiffness, A_{ij} ; lamination parameters, ξ_2, ξ_4 and; effective moduli for a single layer of
21 balanced plain weave, $E_x = E_y = (A_{11}A_{22} - A_{12}^2)/A_{22}t$ and $G_{xy} = A_{66}/t$.
22
23
24
25
26
27
28
29

30 **Figure 3** - Polar plots of the lamination parameters corresponding to: (a) **A** (b) **B** and
31 (c) **D** stiffness properties with off-axis material alignment, $0^\circ \leq \beta \leq 360^\circ$, for 2-ply
32 **A_IB_SD_I** balanced plain weave laminate stacking sequence $[\alpha/\beta]_T$, where $\alpha = \beta + \pi/4$.
33
34
35
36
37
38
39
40

41 **Figure 4** - Polar plots of the lamination parameters for: (a) **A** (b) **B** and (c) **D** matrices
42 corresponding to off-axis material alignment, $0^\circ \leq \beta \leq 360^\circ$, for 3-ply **A_SB_SD_S** laminate
43 stacking sequence $[\alpha/\beta_2]_T$, where $\alpha = \beta + \pi/4$.
44
45
46
47
48
49
50
51

52 **Figure 5** - Polar plots of the lamination parameters for: (a) **A** (b) **B** and (c) **D** matrix
53 corresponding to off-axis material alignment, $0^\circ \leq \beta \leq 360^\circ$, for 6-ply **A_IB_SD_S** laminate
54 stacking sequence $[\alpha/\beta/\alpha_2/\beta_2]_T$, where $\alpha = \beta + \pi/4$.
55
56
57
58
59
60
61
62
63
64
65

Figure 6 - Twist Rate vs Axial Force for the unidirectional and balanced plain weave laminate comparators with equal thickness.

1
2
3
4
5
6
7
8
9
10
11
12
13
14
15
16
17
18
19
20
21
22
23
24
25
26
27
28
29
30
31
32
33
34
35
36
37
38
39
40
41
42
43
44
45
46
47
48
49
50
51
52
53
54
55
56
57
58
59
60
61
62
63
64
65

1
2
3
4 **Tables**
5
6
7
8

9 **Table 1** – Property comparisons for unidirectional and balanced plain weave (Hexcel™)
10
11 intermediate (60% fibre volume) modulus carbon/epoxy materials. Values in
12
13 parentheses indicate compressive moduli.
14
15
16

17

Properties	Unidirectional	Plain Weave
E_1	170 (150) GPa	90 (80) GPa
E_2	9 (11) GPa	90 (80*) GPa
G_{12}	4.4 GPa	5 GPa
ν_{12}	0.27	0.05
t	0.183 mm	0.366 mm
σ_1^T	2,400 MPa	900 MPa
σ_1^C	-1,600 MPa	-800 MPa
σ_2^T	80 MPa	850 MPa
σ_2^C	-250 MPa	-750 MPa
τ_{12}^F	95 MPa	80 MPa

18
19
20
21
22
23
24
25
26
27
28
29
30
31
32
33
34
35
36

37 *Compressive moduli $E_2 = E_1$ assumed instead of published value, $E_2 = 75\text{GPa}$.
38
39
40
41
42
43
44
45
46
47
48
49
50
51
52
53
54
55
56
57
58
59
60
61
62
63
64
65

Table 2 - Square symmetric forms of the Extensional [**A**] and Bending [**D**] stiffness matrices for uncoupled (Simple) with $\beta = m\pi/4$ and coupled behaviour with $\beta \neq m\pi/4$.

Extensional [A]		Bending [D]	
Simple	<u>E-S</u>	Simple	<u>B-T</u>
$[\mathbf{A}_S]$ $\begin{bmatrix} A_{11} & A_{12} & 0 \\ A_{12} & A_{11} & 0 \\ 0 & 0 & A_{66} \end{bmatrix}$ $\xi_4 = 0$	$[\mathbf{A}_F]$ $\begin{bmatrix} A_{11} & A_{12} & A_{16} \\ A_{12} & A_{11} & -A_{16} \\ A_{16} & -A_{16} & A_{66} \end{bmatrix}$	$[\mathbf{D}_S]$ $\begin{bmatrix} D_{11} & D_{12} & 0 \\ D_{12} & D_{11} & 0 \\ 0 & 0 & D_{66} \end{bmatrix}$ $\xi_{12} = 0$	$[\mathbf{D}_F]$ $\begin{bmatrix} D_{11} & D_{12} & D_{16} \\ D_{12} & D_{11} & -D_{16} \\ D_{16} & -D_{16} & D_{66} \end{bmatrix}$

Table 3 - Coupling $[\mathbf{B}]$ stiffness matrices with square symmetry, and associated *cause-effect* relationship, subscript notation and lamination parameter constraints, for coupled behaviour with respect to material axis alignment, β .

$\beta = m\pi/4$	$\beta = \pi/8 + m\pi/4$ ($m = 0, 1, 2, 3, \dots$)	$\beta \neq m\pi/2, \pi/8 + m\pi/4$
<u>$E-B-S-T$</u>	<u>$E-T-S-B$</u>	<u>$E-B-S-B-E-T-S-T$</u>
$[\mathbf{B}_S]$	$[\mathbf{B}_t]$	$[\mathbf{B}_F]$
$\begin{bmatrix} \mathbf{B}_{11} & -\mathbf{B}_{11} & 0 \\ -\mathbf{B}_{11} & \mathbf{B}_{11} & 0 \\ 0 & 0 & -\mathbf{B}_{11} \end{bmatrix}$	$\begin{bmatrix} 0 & 0 & \mathbf{B}_{16} \\ 0 & 0 & -\mathbf{B}_{16} \\ \mathbf{B}_{16} & -\mathbf{B}_{16} & 0 \end{bmatrix}$	$\begin{bmatrix} \mathbf{B}_{11} & -\mathbf{B}_{11} & \mathbf{B}_{16} \\ -\mathbf{B}_{11} & \mathbf{B}_{11} & -\mathbf{B}_{16} \\ \mathbf{B}_{16} & -\mathbf{B}_{16} & -\mathbf{B}_{11} \end{bmatrix}$
$\xi_8 = 0$	$\xi_6 = 0$	

Table 4 – Comparisons of stiffness and compliance matrices for different *cause-effect* relationships. Note that $\alpha = \beta + \pi/4$ in stacking sequence definition.

	$\mathbf{A}_S \mathbf{B}_T \mathbf{D}_S$ laminate: $[\beta_3/\alpha_3]_T$ <u>E-T-S-B</u>	$\mathbf{A}_S \mathbf{B}_T \mathbf{D}_F$ laminate: $[\beta_2/\alpha_2/\beta/\alpha]_T$ <u>E-T-S-B;B-T</u>
Stiffness Matrix	$\begin{bmatrix} A_{11} & A_{12} & 0 & 0 & 0 & B_{16} \\ A_{12} & A_{11} & 0 & 0 & 0 & -B_{16} \\ 0 & 0 & A_{66} & B_{16} & -B_{16} & 0 \\ 0 & 0 & B_{16} & D_{11} & D_{12} & 0 \\ 0 & 0 & -B_{16} & D_{12} & D_{11} & 0 \\ B_{16} & -B_{16} & 0 & 0 & 0 & D_{66} \end{bmatrix}$	$\begin{bmatrix} A_{11} & A_{12} & 0 & 0 & 0 & B_{16} \\ A_{12} & A_{11} & 0 & 0 & 0 & -B_{16} \\ 0 & 0 & A_{66} & B_{16} & -B_{16} & 0 \\ 0 & 0 & B_{16} & D_{11} & D_{12} & D_{16} \\ 0 & 0 & -B_{16} & D_{12} & D_{11} & -D_{16} \\ B_{16} & -B_{16} & 0 & D_{16} & -D_{16} & D_{66} \end{bmatrix}$
Compliance Matrix	$\begin{bmatrix} a_{11} & -a_{12} & 0 & 0 & 0 & b_{16} \\ -a_{12} & a_{11} & 0 & 0 & 0 & -b_{16} \\ 0 & 0 & a_{66} & b_{16} & -b_{16} & 0 \\ 0 & 0 & b_{16} & d_{11} & -d_{12} & 0 \\ 0 & 0 & -b_{16} & -d_{12} & d_{11} & 0 \\ b_{16} & -b_{16} & 0 & 0 & 0 & d_{66} \end{bmatrix}$	$\begin{bmatrix} a_{11} & -a_{12} & a_{16} & b_{11} & -b_{11} & b_{16} \\ -a_{12} & a_{11} & -a_{16} & -b_{11} & b_{11} & -b_{16} \\ a_{16} & -a_{16} & a_{66} & b_{16} & -b_{16} & b_{66} \\ b_{11} & -b_{11} & b_{16} & d_{11} & -d_{12} & d_{16} \\ -b_{11} & b_{11} & -b_{16} & -d_{12} & d_{11} & -d_{16} \\ b_{16} & -b_{16} & b_{66} & d_{16} & -d_{16} & d_{66} \end{bmatrix}$

Table 5 - Summary on the number of Simple, uncoupled ($\mathbf{A}_S\mathbf{B}_0\mathbf{D}_S$) laminates for each ply number grouping, n , and the number that possess **quasi-homogeneous** ($\mathbf{A}_S\mathbf{B}_0\mathbf{D}_S$), fully isotropic ($\mathbf{A}_I\mathbf{B}_0\mathbf{D}_I$) or extensionally isotropic ($\mathbf{A}_I\mathbf{B}_0\mathbf{D}_S$) properties.

n	Simple $\mathbf{A}_S\mathbf{B}_0\mathbf{D}_S$	Quasi-homogeneous $\mathbf{A}_S\mathbf{B}_0\mathbf{D}_S$	Fully Isotropic $\mathbf{A}_I\mathbf{B}_0\mathbf{D}_I$	Extensionally Isotropic $\mathbf{A}_I\mathbf{B}_0\mathbf{D}_S$
2	1	1		
3	2	1		
4	2	1		1
5	4	1		
6	4	1		
7	10	2		
8	9	1	1	3
9	26	1		
10	24	1		
11	76	5		
12	69	1	1	28
13	236	12		
14	214	7		
15	760	12		
16	696	7	7	256
17	2522	53		
18	2326	22		
19	8556	122		
20	7942	67	24	2700
21	29504	99		

Table 6 - Fully isotropic ($A_1B_0D_1$) laminates for each ply number groupings, n , with $\alpha = \beta + \pi/4$.

n	Stacking sequence
8	$[\alpha/\beta_2/\alpha/\beta/\alpha_2/\beta]_T$
12	$[\alpha/\beta/\alpha/\beta_3/\alpha_3/\beta/\alpha/\beta]_T$
16	$[\alpha/\beta_3/\alpha_4/\beta_2/\alpha/\beta_2/\alpha/\beta/\alpha]_T$
	$[\alpha/\beta_2/\alpha/\beta/\alpha_2/\beta_2/\alpha_2/\beta/\alpha/\beta_2/\alpha]_T$
	$[\alpha/\beta_2/\alpha/\beta/\alpha_2/\beta/\alpha/\beta_2/\alpha/\beta/\alpha_2/\beta]_T$
	$[\alpha/\beta_2/\alpha_2/\beta_2/\alpha/\beta/\alpha_2/\beta_2/\alpha_2/\beta]_T$
	$[\alpha/\beta/\alpha/\beta_2/\alpha/\beta_2/\alpha_4/\beta_3/\alpha]_T$
	$[\alpha/\beta/\alpha/\beta_2/\alpha/\beta/\alpha/\beta/\alpha/\beta/\alpha_2/\beta/\alpha/\beta]_T$
	$[\alpha_2/\beta_4/\alpha_2/\beta_2/\alpha_4/\beta_2]_T$
	$[\alpha_2/\beta/\alpha/\beta_5/\alpha/\beta/\alpha_5/\beta/\alpha/\beta_2]_T$
	$[\alpha_2/\beta_2/\alpha/\beta_3/\alpha/\beta/\alpha/\beta/\alpha_3/\beta/\alpha_2/\beta_2]_T$
	$[\alpha_2/\beta_3/\alpha/\beta/\alpha/\beta_2/\alpha_2/\beta/\alpha/\beta/\alpha_3/\beta_2]_T$
	$[\alpha/\beta_2/\alpha_2/\beta/\alpha/\beta/\alpha/\beta_3/\alpha/\beta/\alpha_4/\beta_2]_T$
	$[\alpha/\beta/\alpha_2/\beta_4/\alpha/\beta/\alpha/\beta/\alpha_4/\beta_2/\alpha/\beta]_T$
	$[\alpha/\beta/\alpha/\beta/\alpha/\beta/\alpha/\beta_4/\alpha_5/\beta_2/\alpha/\beta]_T$
	$[\alpha/\beta/\alpha_2/\beta_5/\alpha_4/\beta/\alpha/\beta/\alpha/\beta/\alpha/\beta]_T$
	$[\alpha/\beta/\alpha/\beta/\alpha/\beta_2/\alpha/\beta_2/\alpha_2/\beta/\alpha_2/\beta/\alpha/\beta/\alpha/\beta]_T$
	$[\alpha/\beta/\alpha/\beta_2/\alpha_2/\beta_2/\alpha/\beta_2/\alpha_3/\beta/\alpha/\beta/\alpha/\beta]_T$
$[\alpha/\beta/\alpha/\beta/\alpha/\beta_3/\alpha_2/\beta/\alpha_2/\beta_2/\alpha_2/\beta/\alpha/\beta]_T$	
$[\alpha/\beta/\alpha/\beta_2/\alpha_2/\beta_3/\alpha_3/\beta_2/\alpha_2/\beta/\alpha/\beta]_T$	
20	$[\alpha/\beta/\alpha/\beta_3/\alpha_4/\beta_4/\alpha_3/\beta/\alpha/\beta]_T$
	$[\alpha/\beta_2/\alpha/\beta/\alpha_2/\beta/\alpha/\beta/\alpha/\beta_3/\alpha_3/\beta/\alpha/\beta]_T$
	$[\alpha_2/\beta_4/\alpha/\beta/\alpha_3/\beta/\alpha/\beta/\alpha/\beta_2/\alpha_2/\beta]_T$
	$[\alpha/\beta_2/\alpha_2/\beta/\alpha/\beta_3/\alpha_3/\beta/\alpha/\beta_2/\alpha_2/\beta]_T$
	$[\alpha/\beta/\alpha/\beta_3/\alpha_3/\beta/\alpha/\beta/\alpha/\beta_2/\alpha/\beta/\alpha_2/\beta]_T$
	$[\alpha/\beta_2/\alpha/\beta/\alpha/\beta/\alpha_3/\beta_3/\alpha/\beta/\alpha/\beta/\alpha_2/\beta]_T$
	$[\alpha/\beta_3/\alpha_3/\beta/\alpha_2/\beta_2/\alpha/\beta_3/\alpha_3/\beta]_T$
	$[\alpha/\beta/\alpha/\beta/\alpha/\beta_3/\alpha/\beta/\alpha_4/\beta_2/\alpha/\beta_2/\alpha]_T$
	$[\alpha/\beta/\alpha/\beta_3/\alpha_3/\beta/\alpha/\beta_2/\alpha_2/\beta/\alpha/\beta_2/\alpha]_T$
	$[\alpha_2/\beta_5/\alpha_5/\beta/\alpha/\beta_3/\alpha/\beta/\alpha]_T$
$[\alpha/\beta_2/\alpha/\beta/\alpha_2/\beta_2/\alpha/\beta/\alpha_3/\beta_3/\alpha/\beta/\alpha]_T$	
$[\alpha/\beta_2/\alpha/\beta_2/\alpha_4/\beta/\alpha/\beta_3/\alpha/\beta/\alpha/\beta/\alpha]_T$	
$[\alpha/\beta/\alpha/\beta_3/\alpha/\beta/\alpha_5/\beta_5/\alpha_2]_T$	

Table 7 - Classification of coupled laminates with balance plain weave, derived from the $A_S B_t D_S$ parent laminate with Bending-Extension and Twisting-Shearing ($B-E-T-S$) coupling, following off-axis material alignment, β . Illustrations highlight the coupling responses due to free thermal contraction in unbalanced plain weave. For stacking sequence definition, $\alpha = \beta + \pi/4$.

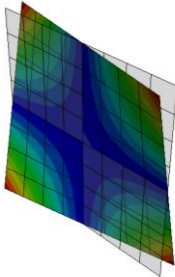
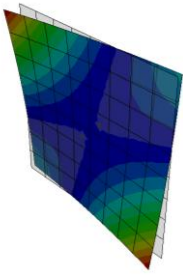
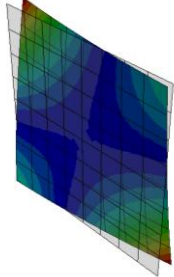
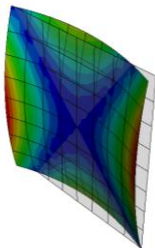
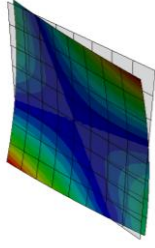
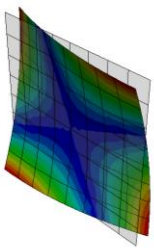
Uncoupled in Extension [A_S]		Extension-Shearing [A_F]	
Uncoupled in Bending [D_S]	Bending-Twisting [D_F]	Bending-Twisting [D_F]	
$A_S B_t D_S$ $[\alpha/\beta]_T$  <u>$B-S-T-E$</u>	$A_S B_t D_F$ $[\alpha/\beta/\alpha_2/\beta_2]_T$  <u>$B-S-T-E; B-T$</u>	$A_F B_t D_F$ $[\alpha/\beta_2]_T$  <u>$E-S; B-S-T-E; B-T$</u>	$\beta = \pi/8 + m\pi/4$ ($m = 0, 1, 2, \dots$) Bending-Shearing and Twisting-Extension [B_t]
$A_S B_f D_S$ $[\alpha/\beta]_T$  <u>$B-E-B-S-T-E-T-S$</u>	$A_S B_f D_F$ $[\alpha/\beta/\alpha_2/\beta_2]_T$  <u>$B-E-B-S-T-E-T-S; B-T$</u>	$A_F B_f D_F$ $[\alpha/\beta_2]_T$  <u>$E-S; B-E-B-S-T-E-T-S; B-T$</u>	

Table 8 - Number of solutions for the E-B-S-T or B-E-T-S coupled parent ($A_S B_S D_S$) laminate class for each ply number grouping, n , and number of solutions in each of the six other coupled laminate derivatives of Table 7, following off-axis alignment, β .

n	Number of solutions						
	$A_S B_S D_S$	$A_S B_T D_S$	$A_S B_T D_F$	$A_F B_T D_F$	$A_S B_F D_S$	$A_S B_F D_F$	$A_F B_F D_F$
	$\beta = 0$	$\beta = \pi/8 + m\pi/4$ ($m = 0, 1, 2, 3, \dots$)			$\beta \neq m\pi/4, \pi/8 + m\pi/2$ ($m = 0, 1, 2, 3, \dots$)		
2	1	1			1		
3	2			2			2
4	6	2		4	2		4
5	12			12			12
6	28	4	6	18	4	6	18
7	54			54			54
8	119	7	24	88	7	24	88
9	230			230			230
10	488	16	110	362	16	110	362
11	948			948			948
12	1979	35	398	1546	35	398	1546
13	3860			3860			3860
14	7978	84	1632	6262	84	1632	6262
15	15624			15624			15624
16	32072	194	5978	25900	194	5978	25900
17	63014			63014			63014
18	128746	512	23798	104436	512	23798	104436
19	253588			253588			253588
20	516346	1352	88302	426692	1352	88302	426692
21	1019072			1019072			1019072

Appendix

Table A1 - Subscript notation, response based labelling and associated form of the: (a) extensional stiffness matrix, $[\mathbf{A}]$; (b), bending stiffness matrix, $[\mathbf{D}]$ and; (c) coupling stiffness matrix, $[\mathbf{B}]$. Note that all stiffness matrices have square symmetric form for balanced plain weave material. Note also that the A_I and D_I are used in place of A_S and D_S to denote isotropic stiffness relationships as defined in Eqs (14) and (15).

(a)

Subscript notation (ESDU, 1994)	Response-based labelling	Matrix form
\mathbf{A}_S	Simple laminate	$\begin{bmatrix} A_{11} & A_{12} & 0 \\ A_{12} & A_{11} & 0 \\ 0 & 0 & A_{66} \end{bmatrix}$
\mathbf{A}_F	Shear-Extension; <u>S-E</u>	$\begin{bmatrix} A_{11} & A_{12} & A_{16} \\ A_{12} & A_{11} & -A_{16} \\ A_{16} & -A_{16} & A_{66} \end{bmatrix}$

(b)

Subscript notation (ESDU, 1994)	Response-based labelling	Matrix form
\mathbf{D}_S	Simple laminate	$\begin{bmatrix} D_{11} & D_{12} & 0 \\ D_{12} & D_{11} & 0 \\ 0 & 0 & D_{66} \end{bmatrix}$
\mathbf{D}_F	Twisting-Bending; <u>T-B</u>	$\begin{bmatrix} D_{11} & D_{12} & D_{16} \\ D_{12} & D_{11} & -D_{16} \\ D_{16} & -D_{16} & D_{66} \end{bmatrix}$

(c)

Subscript notation (ESDU, 1994)	Response-based labelling	Matrix form
\mathbf{B}_t	Extension-Twisting and Shearing-Bending; <u>E-T-S-B</u>	$\begin{bmatrix} 0 & 0 & B_{16} \\ 0 & 0 & -B_{16} \\ B_{16} & -B_{16} & 0 \end{bmatrix}$
\mathbf{B}_s	Extension-Bending and Shearing-Twisting; <u>E-B-S-T</u>	$\begin{bmatrix} B_{11} & -B_{11} & 0 \\ -B_{11} & B_{11} & 0 \\ 0 & 0 & -B_{11} \end{bmatrix}$
\mathbf{B}_F	Extension-Bending, Shearing-Bending, Extension-Twisting, and Shearing-Twisting; <u>E-B-S-B-E-T-S-T</u>	$\begin{bmatrix} B_{11} & -B_{11} & B_{16} \\ -B_{11} & B_{11} & -B_{16} \\ B_{16} & -B_{16} & -B_{11} \end{bmatrix}$

Table A2 - Abridged listing for Simple laminates ($\mathbf{A}_s\mathbf{B}_0\mathbf{D}_s$), corresponding to $\beta = 0$ and $\alpha = \beta + \pi/4$, for increasing buckling strength of the infinitely long plate with simply supported edges. Note that for ply number groupings $n = 4$ and above, the maximum buckling strength arises from stacking sequences of the form $[\alpha_n]_T$, corresponding to lamination parameter $\xi_2 = \xi_8 = -1$ with $k_x = 5.06$ and corresponding buckling half-wavelength $\lambda = b$.

n	Stacking Sequences	ξ_2	ξ_{10}	k_x
2	$[\alpha/\alpha]_T$	-1.00	-1.00	5.06
3	$[\alpha/\beta/\alpha]_T$	-0.33	-0.93	4.98
3	$[\alpha_3]_T$	-1.00	-1.00	5.06
4	$[\alpha/\beta_2/\alpha]_T$	0.00	-0.75	4.80
:				
5	$[\alpha/\beta_3/\alpha]_T$	0.20	-0.57	4.60
:				
6	$[\alpha/\beta_4/\alpha]_T$	0.33	-0.41	4.43
:				
7	$[\alpha/\beta_3/\alpha_2/\beta]_T$	0.14	0.00	4.00
:				
8	$[\alpha/\beta_2/\alpha/\beta/\alpha_2/\beta]_T$	0.00	0.00	4.00
:				
9	$[\alpha/\beta_4/\alpha/\beta/\alpha/\beta]_T$	0.33	0.14	3.86
:				
10	$[\alpha/\beta_4/\alpha_3/\beta_2]_T$	0.20	0.30	3.69
:				
11	$[\alpha/\beta_6/\alpha_2/\beta_2]_T$	0.46	0.31	3.68
:				
12	$[\alpha/\beta_5/\alpha_2/\beta/\alpha/\beta_2]_T$	0.33	0.37	3.61
:				
13	$[\alpha/\beta_6/\alpha_3/\beta_3]_T$	0.39	0.45	3.52
:				
14	$[\alpha/\beta_6/\alpha/\beta/\alpha_2/\beta_3]_T$	0.43	0.46	3.51
:				
15	$[\alpha/\beta_7/\alpha_2/\beta/\alpha/\beta_3]_T$	0.47	0.50	3.47
:				
16	$[\alpha/\beta_8/\alpha_3/\beta_4]_T$	0.50	0.54	3.42
:				
17	$[\alpha/\beta_8/\alpha/\beta/\alpha_2/\beta_4]_T$	0.53	0.56	3.41
:				

1
2
3
4
5
6
7
8
9
10
11
12
13
14
15
16
17
18
19
20
21
22
23
24
25
26
27
28
29
30
31
32
33
34
35
36
37
38
39
40
41
42
43
44
45
46
47
48
49
50
51
52
53
54
55
56
57
58
59
60
61
62
63
64
65

18	$[\alpha/\beta_9/\alpha_2/\beta/\alpha/\beta_4]_{\Gamma}$	0.56	0.58	3.38
	:			
19	$[\alpha/\beta_{10}/\alpha_3/\beta_5]_{\Gamma}$	0.58	0.61	3.35
	:			
20	$[\alpha/\beta_{10}/\alpha/\beta/\alpha_2/\beta_5]_{\Gamma}$	0.60	0.62	3.34
	:			
21	$[\alpha/\beta_{10}/\alpha_4/\beta_6]_{\Gamma}$	0.52	0.66	3.30

Table A3 - Abridged listing for Extension-Twisting and Shearing-Bending coupled laminates ($\mathbf{A}_1\mathbf{B}_1\mathbf{D}_1$), corresponding to $\beta = \pi/8$ and $\alpha = \beta + \pi/4$, for increasing coupling magnitude, ξ_8 , and corresponding buckling factor k_x for the infinitely long plate with simply supported edges. For ply number groupings above $n = 6$, the maximum coupling magnitude ($\xi_8 = 1$ and $k_x = 3.40$) arises from stacking sequences of the form $[\alpha_{n/2}/\beta_{n/2}]_T$, and are therefore omitted.

n	Stacking Sequences	ξ_8	k_x
2	$[\alpha/\beta]_T$	1.00	3.40
4	$[\alpha/\beta/\alpha/\beta]_T$	0.50	3.85
4	$[\alpha_2/\beta_2]_T$	1.00	3.40
6	$[\alpha/\beta_2/\alpha_2/\beta]_T$	0.11	3.99
:	:	:	
6	$[\alpha_3/\beta_3]_T$	1	3.40
8	$[\alpha/\beta_3/\alpha_3/\beta]_T$	-0.13	3.99
:	:	:	
10	$[\alpha/\beta_2/\alpha_2/\beta_2/\alpha_2/\beta]_T$	0.04	3.99
:	:	:	
12	$[\alpha/\beta_2/\alpha_2/\beta/\alpha/\beta_2/\alpha_2/\beta]_T$	0.06	3.99
:	:	:	
14	$[\alpha/\beta_2/\alpha/\beta/\alpha_2/\beta/\alpha/\beta/\alpha/\beta_2/\alpha]_T$	0.02	4.00
:	:	:	
16	$[\alpha/\beta_2/\alpha/\beta/\alpha_3/\beta_3/\alpha/\beta/\alpha_2/\beta]_T$	0.03	4.00
:	:	:	
18	$[\alpha/\beta_3/\alpha_4/\beta_2/\alpha/\beta/\alpha/\beta_2/\alpha/\beta/\alpha]_T$	0.01	4.00
:	:	:	
20	$[\alpha/\beta_3/\alpha_2/\beta/\alpha_4/\beta_3/\alpha/\beta_3/\alpha_2]_T$	0.02	4.00
:	:	:	